Contemporary Mathematics
https://ojs.wiserpub.com/index.php/CM/

Research Article

A Fractal-Fractional Approach to Non-linear Predator-Prey Models with Logistic Growth, Holling Type II Functional Response and Immigration Effects

Abdelkader Moumen[1], Arshad Ali[2†], Khaled Aldwoah[3*], Hicham Saber[1], Tariq A. Alraqad[1], Alaa M. Abd El-latif[4], Etaf Alshawarbeh[1]

[1] Department of Mathematics, College of Science, University of Hail, Hail, 55473, Saudi Arabia
[2] Department of Mathematics, University of Malakand, Lower Dir, Khyber Pakhtunkhwa, 18000, Pakistan
[3] Department of Mathematics, Faculty of Science, Islamic University of Madinah, Madinah, 42351, Saudi Arabia
[4] Mathematics Department, College of Science, Northern Border University, Arar, 91431, Saudi Arabia
E-mail: arshad.swatpk@gmail.com; aldwoah@iu.edu.sa

Received: 13 October 2025; **Revised:** 19 November 2025; **Accepted:** 27 November 2025

Abstract: This paper develops a nonlinear fractal-fractional predator-prey model that incorporates logistic prey growth and immigration effects. The predator-prey interaction is characterized by a Holling type II functional response, capturing the saturation phenomenon in the predator's feeding rate. Using the Caputo-Fabrizio (CF) fractional operator, the model integrates memory effects into the population dynamics. Theoretical investigations establish the existence and uniqueness of solutions by applying Krasnoselskii's fixed point theorem and Banach's contraction principle, followed by the stability analysis of equilibrium points. For the numerical approximation, a modified Adams-Bashforth method adapted to the CF operator is employed. Simulation results reveal that small yet positive immigration rates promote asymptotically stable coexistence between prey and predator populations, emphasizing the stabilizing influence of immigration on ecosystem dynamics. The study demonstrates how fractal-fractional calculus can provide deeper insight into ecological stability and long-term behavior of interacting species.

***Keywords*:** Fractal-Fractional Caputo-Fabrizio (FFCF) operator, predator-prey model, Holling type II functional response, logistic growth, immigration effects, stability analysis, fixed point results, numerical simulation

MSC: 45G15, 45M99

1. Introduction

Eco-epidemiology is an interdisciplinary field that investigates infectious disease dynamics within ecological systems by examining interactions among hosts, pathogens, and their environments. It connects ecology and epidemiology, offering insights into how biological and environmental factors influence population-level outcomes. The mathematical modeling of such systems provides a framework for understanding and predicting complex population dynamics.

The classical Lotka-Volterra model [1] laid the foundation for analyzing predator-prey interactions, later extended to include features such as interspecific competition, time delays, and nonlinear functional responses [2–5]. These

DOI: https://doi.org/10.37256/cm.7120268879

developments have significantly advanced the study of ecological systems, including their stability and oscillatory behavior. In parallel, mathematical models have become essential tools in epidemiology, particularly through compartmental formulations such as the Susceptible-Infected-Recovered (SIR) model [6]. Researchers have increasingly integrated disease transmission mechanisms into predator-prey frameworks, recognizing that infection can alter prey vulnerability and predator feeding behavior [7–13]. Such eco-epidemiological models capture biologically realistic features but often rely on classical differential equations, which neglect memory and hereditary effects.

Fractional-order differential equations have emerged as powerful tools for modeling processes influenced by memory and non-locality. Their applications span various scientific fields, including control theory [14], electrical circuits [15], robotics [16], materials science [17], and biological systems [18–21]. Recently, there have also been important advances in numerical spectral methods for fractional dynamics. For example, Youssri et al. proposed an innovative pseudo-spectral Galerkin algorithm for the time-fractional Tricomi-type equation [22]; similarly, Youssri et al. introduced a Chebyshev Petrov-Galerkin method for nonlinear time-fractional integro-differential equations with a mildly singular kernel [23]. Furthermore, Abd-Elhameed et al. developed an orthogonal-Chebyshev spectral scheme for the fractional Rayleigh-Stokes problem [24]. These recent works illustrate the rapid development of efficient and accurate numerical tools in the fractional calculus literature.

On the theoretical side, development of fractional operators-such as the conformable derivative [25], the Caputo difference operator [26], and the Caputo-Fabrizio (CF) derivative [27]-has further enriched the modeling landscape. In particular, Atangana [28] introduced the concept of the fractal-fractional derivative, a hybrid operator that combines the local behavior of fractal geometry with the memory properties of fractional calculus. This operator has been successfully used to describe complex natural processes characterized by self-similarity and memory dependence [29–33], especially in ecological contexts where heterogeneity and history significantly influence dynamic behavior.

In ecological modeling, several recent studies have incorporated immigration effects to reflect the movement of individuals across populations. For instance, [34] analyzed a predator-prey model with immigration using classical differential equations, while [35] extended this formulation through the fractal-fractional CF operator. Although these models provide valuable insights, they rely on certain idealizations, such as exponential prey growth and linear predation rates, which may limit their ecological realism-because exponential growth neglects environmental constraints, and linear predation fails to reflect predator saturation. In particular, exponential growth ignores environmental constraints, and linear predation fails to capture predator saturation. To address these limitations, the present study develops a nonlinear fractal-fractional predator-prey model that integrates logistic prey growth and a Holling type II functional response, thereby introducing both environmental carrying capacity and nonlinear predator behavior. The proposed system is governed by the fractal-fractional CF operator, defined as:

$$\begin{cases} {}^{\mathrm{FFCF}}D^{\kappa_1,\,\kappa_2}\Phi(t) = r\Phi(t)\left(1-\dfrac{\Phi(t)}{\varsigma}\right) - \dfrac{a\Phi(t)\Psi(t)}{1+h\Phi(t)} + \mathscr{P}(\Phi), \\ {}^{\mathrm{FFCF}}D^{\kappa_1,\,\kappa_2}\Psi(t) = \dfrac{b\Phi(t)\Psi(t)}{1+h\Phi(t)} - m\Psi(t) + \mathscr{Q}(\Psi). \end{cases} \tag{1}$$

In this model, Φ represents the population size of the prey species, while Ψ corresponds to the population size of the predator species. The parameter r signifies the intrinsic growth rate of the prey population. The predation rate, denoted by a, quantifies the rate at which predators consume prey. The parameter b characterizes the predator's reproductive efficiency, measuring the number of new predators produced per prey captured. Meanwhile, m represents the natural mortality rate of the predator population, ς is the environmental carrying capacity for the prey population, h is the handling time per prey item (Holling type II response). In the proposed model, the logistic growth of the prey population account for environmental carrying capacity and resource competition. While the nonlinear (Holling Type II) functional response reflects the saturation effect in predation due to handling time. Table 1 provides a summary of all parameter values.

Table 1. Description and biological interpretation of the model parameters

Parameter	Biological interpretation	Typical range	Source
r	Intrinsic growth rate of the prey population	0.1	[35]
a	Predation rate coefficient	0.1	[35]
b	Predator's reproductive efficiency	0.3	[35]
m	Natural mortality rate of predators	0.2	[35]
ς	Environmental carrying capacity for prey	1,000 individuals	Assumed
h	Handling time per prey item (Holling type II response)	0.01	Assumed
x	Immigration rate of prey	0-0.01	[35]
z	Immigration rate of predators	0-0.01	[35]

The immigration function can be represented by the following two ways [34, 35]:

$$\mathscr{P}(\Phi) = \begin{cases} x,\ x \geq 0, \\ \\ x/\Phi,\ x > 0, \end{cases}$$

where x denotes the prey population influx due to immigrants, and x/Φ signifies the proportion of immigrants within the prey population. Similarly,

$$\mathscr{Q}(\Psi) = \begin{cases} z,\ z \geq 0, \\ \\ z/\Psi,\ z > 0, \end{cases}$$

where z denotes the prey population influx due to immigrants, and z/Ψ signifies the proportion of immigrants within the prey population.

The key novel contributions of this study are summarized as follows:

• Introduction of a fractal-fractional predator-prey model with logistic growth and Holling type II response under immigration influence.

• Establishment of existence and uniqueness results using Krasnoselskii's fixed point theorem and Banach's contraction principle within the CF framework.

• Examination of stability properties and numerical dynamics using a modified Adams-Bashforth method adapted for the fractal-fractional operator.

• Demonstration, through simulations, that small positive immigration rates enhance coexistence stability between predator and prey.

The remainder of this paper is organized as follows: Section 2 explores equilibrium points and their stability. Preliminary theoretical results are presented in Section 3. Existence and uniqueness of solutions are established in Section 4. Section 5 presents the numerical scheme used for simulations. In Section 6, simulation outcomes are analyzed using selected parameter values. Final conclusions are provided in Section 7.

2. Equilibrium points and their stability analysis

The trivial equilibrium of the model does exist in case the immigration terms are not zero. Similarly, the prey only equilibrium $(\Phi^*,\ 0)$ is not admissible in the presence of predator immigration $z > 0$. The only admissible equilibrium is the coexistence equilibrium $(\Phi^*,\ \Psi^*)$ whose numerical value is calculated for the given parameter values as $(0.641695,\ 1.146925)$.

Now, to analyze its stability, we find the Jacobian matrix of the proposed model as below.

$$J = \begin{bmatrix} \dfrac{\partial f_1}{\partial \Phi} & \dfrac{\partial f_1}{\partial \Psi} \\ \dfrac{\partial f_2}{\partial \Phi} & \dfrac{\partial f_2}{\partial \Psi} \end{bmatrix}. \tag{2}$$

Taking the partial derivatives, we obtain

$$J = \begin{bmatrix} \dfrac{(\Psi\Phi aq)}{(\Phi q+1)^2} - r(\dfrac{\Phi}{K}-1) - \dfrac{(\Phi r)}{K} - \dfrac{(\Psi a)}{(\Phi q+1)} - \dfrac{c}{\Phi^2} & -\dfrac{(\Phi a)}{(\Phi q+1)} \\ \dfrac{(\Psi b)}{(\Phi q+1)} - \dfrac{(\Psi\Phi bq)}{(\Phi q+1)^2} & \dfrac{(\Phi b)}{(\Phi q+1)} - \dfrac{d}{\Psi^2} - m \end{bmatrix}. \tag{3}$$

Using the parameter values, we obtain the following numerical Jacobian matrix

$$J = \begin{bmatrix} -0.0352 & -0.0638 \\ 0.3397 & -0.0163 \end{bmatrix}. \tag{4}$$

The corresponding eigenvalues are: $-0.0258 + 0.1469i$, $-0.0258 - 0.1469i$.

We observe that the real parts of both eigenvalues are negative. Therefore, the coexistence equilibrium point is locally asymptotically stable.

3. Elementary results

The upcoming section provides essential theoretical foundations and analytical techniques. It includes key concepts from fractal-fractional calculus.

Definition 1 [28] Let $\vartheta(t)$ be a continuous function that is fractally differentiable over the interval $(a,\ b)$ with fractal order κ_2. The fractal-fractional CF derivative of order κ_1 using an exponential decay kernel is defined by:

$${}^{\text{FFCF}}D^{\kappa_1,\,\kappa_2}\vartheta(t) = \frac{M(\kappa_1)}{1-\kappa_1}\int_0^t \frac{d}{d\omega_2^{\kappa}}\vartheta(\omega)\exp\left(-\frac{\kappa_1}{1-\kappa_1}(t-\omega)\right)d\omega, \quad t \in [0,\ T], \tag{5}$$

where $0 < \kappa_1,\ \kappa_2 \leq 1$, and $M(\kappa_1)$ is a normalization function such that $M(0) = M(1) = 1$.

Definition 2 [28] Suppose $\vartheta(t)$ is continuous and fractally differentiable on $(a,\ b)$ with order κ_2. Its Fractal-Fractional Caputo-Fabrizio (FFCF) derivative of order κ_1 with a power-law kernel is given by:

$$^{\mathrm{FFCF}}D^{\kappa_1,\,\kappa_2}\vartheta(t)=\frac{1}{\Gamma(1-\kappa_1)}\int_0^t\frac{d}{d\omega_2^{\kappa}}\vartheta(\omega)(t-\omega)^{-\kappa_1}d\omega,\quad t\in[0,\,T],\tag{6}$$

where $0<\kappa_1,\ \kappa_2\leq 1$, and the fractal derivative is defined as:

$$\frac{d}{d\omega_2^{\kappa}}\vartheta(\omega)=\lim_{t\to\omega}\frac{\vartheta(t)-\vartheta(\omega)}{t^{\kappa_2}-\omega^{\kappa_2}}.\tag{7}$$

Definition 3 [28] Let $\vartheta\in C(0,\ T)$. The Fractal-Fractional Riemann-Liouville (FFRL) integral of $\vartheta(t)$ with an exponential decay kernel is given by:

$$^{\mathrm{FFRL}}I^{\kappa_1,\,\kappa_2}\vartheta(t)=\frac{\kappa_2(1-\kappa_1)t^{\kappa_2-1}\vartheta(t)}{M(\kappa_1)}+\frac{\kappa_1\kappa_2}{M(\kappa_1)}\int_a^t\omega^{\kappa_1-1}\vartheta(\omega)d\omega.\tag{8}$$

Definition 4 [28] Let $\vartheta\in C(0,\ T)$. The FFRL integral of $\vartheta(t)$ using a power-law kernel is defined as:

$$^{\mathrm{FFRL}}I^{\kappa_1,\,\kappa_2}\vartheta(t)=\frac{\kappa_2}{\Gamma(\kappa_1)}\int_a^t(t-\omega)^{\kappa_1-1}\omega^{\kappa_2-1}\vartheta(\omega)d\omega.\tag{9}$$

Theorem 1 [36] Let $(\mathbb{X},\ \|\cdot\|)$ be a Banach space and $\mathfrak{B}$ a nonempty, closed, and convex subset of $\mathbb{X}$. Suppose two operators $\mathbb{Q}_1$ and $\mathbb{Q}_2$ map $\mathfrak{B}$ into $\mathbb{X}$ such that:

- For all $x,\ y\in\mathfrak{B}$, the combination $\mathbb{Q}_1x+\mathbb{Q}_2y$ lies in $\mathbb{X}$;
- The operator $\mathbb{Q}_1$ is a contraction;
- The operator $\mathbb{Q}_2$ is continuous and compact.

Then there exists at least one element $z\in\mathfrak{B}$ such that:

$$z=\mathbb{Q}_1z+\mathbb{Q}_2z.$$

4. Existence theory of model (1)

In this section, we explore the existence of a solution to the proposed system using a fixed-point technique. Let the interval $[0,\ T]$ be denoted as $\mathbb{I}$, and define the Banach space:

$$\mathfrak{B}=C\left(\mathbb{I},\ \mathbb{R}^+\right)\times C\left(\mathbb{I},\ \mathbb{R}^+\right),$$

equipped with the norm:

$$\|\vartheta\|=\max\left\{|\Phi(t)|+|\Psi(t)|\right\}.$$

Let

$$\begin{cases} g_1(t,\ \Phi(t),\ \Psi(t)) = r\Phi(t)\left(1-\dfrac{\Phi(t)}{\varsigma}\right) - \dfrac{a\Phi(t)\Psi(t)}{1+h\Phi(t)} + \mathscr{P}(\Phi), \\ \\ g_2(t,\ \Phi(t),\ \Psi(t)) = \dfrac{b\Phi(t)\Psi(t)}{1+h\Phi(t)} - m\Psi(t) + \mathscr{Q}(\Psi). \end{cases} \tag{10}$$

The system is rewritten compactly as:

$$^{\mathrm{FFCF}}D^{\kappa_1,\ \kappa_2}\vartheta(t) = \Theta(t,\ \vartheta(t)). \tag{11}$$

Or

$$^{\mathrm{CF}}D^{\kappa_1}\vartheta(t) = \kappa_2 t^{\kappa_2-1}\Theta(t,\ \vartheta(t)), \tag{12}$$

where the vector $\vartheta(t) = (\Phi,\ \Psi)$, and Θ is expressed as

$$\Theta(t,\ \vartheta(t)) = \begin{bmatrix} g_1(t,\ \Phi,\ \Psi) \\ \\ g_2(t,\ \Phi,\ \Psi) \end{bmatrix}, \tag{13}$$

$$\vartheta(t) = \begin{bmatrix} \Phi(t) \\ \\ \Psi(t) \end{bmatrix} = \begin{bmatrix} r\Phi(t)\left(1-\dfrac{\Phi(t)}{\varsigma}\right) - \dfrac{a\Phi(t)\Psi(t)}{1+h\Phi(t)} + \mathscr{P}(\Phi) \\ \\ \dfrac{b\Phi(t)\Psi(t)}{1+h\Phi(t)} - m\Psi(t) + \mathscr{Q}(\Psi) \end{bmatrix}. \tag{14}$$

Applying the CF fractional integral to (12), we obtain:

$$\vartheta(t) = \Phi(0) + \frac{\kappa_2 t^{\kappa_2-1}(1-\kappa_1)}{\mathscr{M}(\kappa_1)}\Theta(t,\ \vartheta(t)) + \frac{\kappa_1\kappa_2}{\mathscr{M}(\kappa_1)}\int_0^t s^{\kappa_2-1}\Theta(t,\ \vartheta(t))ds. \tag{15}$$

Define the operator $\mathscr{Z} : \mathfrak{B} \to \mathfrak{B}$ by

$$\mathscr{Z}(\vartheta) = \vartheta(t) = \Phi(0) + \frac{\kappa_2 t^{\kappa_2-1}(1-\kappa_1)}{\mathscr{M}(\kappa_1)}\Theta(t,\ \vartheta(t)) + \frac{\kappa_1\kappa_2}{\mathscr{M}(\kappa_1)}\int_0^t s^{\kappa_2-1}\Theta(t,\ \vartheta(t))ds. \tag{16}$$

We assume:
(A_1) There exists $L_\Theta > 0$ such that for all $\vartheta,\ \overline{\vartheta} \in \mathfrak{B}$,

$$|\Theta(t,\ \vartheta(t)) - \Theta(t,\ \overline{\vartheta}(t))| \leq L_\Theta |\vartheta - \overline{\vartheta}|.$$

(A_2) There exist constants $C_\Theta > 0$ and $M_\Theta > 0$ such that

$$|\Theta(t,\ \vartheta(t))| \leq C_\Theta |\vartheta(t)| + M_\Theta.$$

Theorem 2 Under the assumptions (A_1)-(A_2), problem (11) admits at least one solution.
Proof. We express the system as the fixed-point problem $\vartheta = \mathscr{Z}(\vartheta)$. Consider the closed ball:

$$\Omega_\delta = \{\vartheta \in \mathfrak{B} : \|\vartheta\| \leq \delta\},$$

with

$$\delta \geq \frac{|\vartheta_0| + \dfrac{M_\Theta \kappa_2}{M(\kappa_1)} \left((1-\kappa_1)T^{\kappa_2 - 1} + T^{\kappa_1}\right)}{1 - \dfrac{C_\Theta \kappa_2}{M(\kappa_1)} \left((1-\kappa_1)T^{\kappa_2 - 1} + T^{\kappa_1}\right)}.$$

Define $\mathscr{Z} = \mathscr{Z}_1 + \mathscr{Z}_2$ where:

$$\mathscr{Z}_1 \vartheta(t) = \begin{cases} \vartheta_0 + \dfrac{\kappa_2 (1-\kappa_1) t^{\kappa_2 - 1} \Theta(t,\ \vartheta(t))}{M(\kappa_1)}, \end{cases} \tag{17}$$

and

$$\mathscr{Z}_2 \vartheta(t) = \begin{cases} \dfrac{\kappa_1 \kappa_2}{M(\kappa_1)} \displaystyle\int_0^t \omega^{\kappa_1 - 1} \Theta(t,\ \vartheta(t)) d\omega. \end{cases} \tag{18}$$

Several steps are involved in accomplishing the proof.
Step 1: $\mathscr{Z}_1 \vartheta(t) + \mathscr{Z}_2 \vartheta(t) \in \Omega_\delta$. For $t \in \mathbb{I}$, $\vartheta \in \Omega_\delta$, with (A_2), we have

$$\begin{aligned} |\mathscr{Z}_1 \vartheta\,(t) + \mathscr{Z}_2 \vartheta\,(t)| &= \left| \vartheta(t_0) + \frac{\kappa_2 (1-\kappa_1) t^{\kappa_2 - 1} \Theta(t,\ \vartheta(t))}{M(\kappa_1)} + \frac{\kappa_1 \kappa_2}{M(\kappa_1)} \int_0^t \omega^{\kappa_1 - 1} \Theta(t,\ \vartheta(t)) d\omega \right| \\ &\leq |\vartheta_0| + \frac{\kappa_2 (1-\kappa_1) t^{\kappa_2 - 1} |\Theta(t,\ \vartheta(t))|}{M(\kappa_1)} + \frac{\kappa_1 \kappa_2}{M(\kappa_1)} \int_0^t \omega^{\kappa_1 - 1} |\Theta(t,\ \vartheta(t))| d\omega \\ &\leq |\vartheta_0| + \frac{M_\Theta \kappa_2}{M(\kappa_1)} \left((1-\kappa_1)T^{\kappa_2 - 1} + T^{\kappa_1}\right) + \frac{C_\Theta \kappa_2}{M(\kappa_1)} \left((1-\kappa_1)T^{\kappa_2 - 1} + T^{\kappa_1}\right) \delta \leq \delta. \end{aligned} \tag{19}$$

Hence $\mathscr{Z}_1\vartheta(t)+\mathscr{Z}_2\vartheta(t)\in\Omega_\delta$.

Step 2: $\mathscr{Z}_1$ is contraction.

For $t\in\mathbb{I},\ \vartheta_1,\ \vartheta_2\in\Omega_\delta$. Then

$$
\begin{aligned}
|\mathscr{Z}_1\vartheta_1(t)-\mathscr{Z}_1\vartheta_2(t)| &= \max_{t\in[0,\,T]}\left(|\vartheta_1(t_1)-\vartheta_2(t_1)|+\frac{\kappa_2(1-\kappa_1)t^{\kappa_2-1}}{M(\kappa_1)}\,|\Theta(t,\ \vartheta_1(t))-\Theta(t,\ \vartheta_2(t))|\right)\\
&\leq\left(1+\frac{\kappa_2(1-\kappa_1)T^{\kappa_2-1}L_\Theta}{M(\kappa_1)}\right)\|\vartheta_1-\vartheta_2\|,
\end{aligned}
\tag{20}
$$

if $1+\dfrac{\kappa_2(1-\kappa_1)T^{\kappa_2-1}L_\Theta}{M(\kappa_1)}\leq 1$ then $\mathscr{Z}_1$ is contraction.

Step 3: In this step, we will show the relative compactness of $\mathscr{Z}_2$. Consequently, we will show that $\mathscr{Z}_2$ is continuous, uniformly bounded on Ω_δ and equi-continuous.

$\mathscr{Z}_2$ is continuous due to the continuity of $\Theta(t,\ \vartheta(t))$.

$\mathscr{Z}_2$ is uniformly bounded on Ω_δ:

For $t\in\mathbb{I},\ \vartheta\in\Omega_\delta$, we consider

$$
\begin{aligned}
|\mathscr{Z}_2\vartheta(t)| &= \frac{\kappa_1\kappa_2}{M(\kappa_1)}\int_0^t\omega^{\kappa_1-1}\,|\Theta(t,\ \vartheta(t))|\,d\omega\\
&\leq(C_\Theta|\delta|+M_\Theta)\,\frac{\kappa_2}{M(\kappa_1)}T^{\kappa_1}\leq\delta.
\end{aligned}
\tag{21}
$$

Thus $\mathscr{Z}_2$ is uniformly bounded on Ω_δ.

Next, we need to establish equi-continuity.

Let $t_a,\ t_b\in\mathbb{I}$ with $t_a<t_b$. Then

$$
\begin{aligned}
\|\mathscr{Z}_2\vartheta(t_b)-\mathscr{Z}_2\vartheta(t_a)\| &\leq\frac{\kappa_1\kappa_2}{M(\kappa_1)}\int_0^{t_b}\omega^{\kappa_2-1}\,|\Theta(\omega,\ \vartheta(\omega))|\,d\omega-\frac{\kappa_1\kappa_2}{M(\kappa_1)}\int_0^{t_a}\omega^{\kappa_2-1}\,|\Theta(\omega,\ \vartheta(\omega))|\,d\omega\\
&\leq\frac{\kappa_1\kappa_2}{M(\kappa_1)}\left(\int_0^{t_b}\omega^{\kappa_2-1}\,|\Theta(\omega,\ \vartheta(\omega))|\,d\omega-\int_0^{t_a}\omega^{\kappa_2-1}\,|\Theta(\omega,\ \vartheta(\omega))|\,d\omega\right)\\
&=\frac{\kappa_1}{M(\kappa_1)}\left((t_b)^{\kappa_2}-(t_a)^{\kappa_2}\right)(C_\Theta\delta+M_\Theta)\\
&\to 0\text{ as }t_b\to t_a.
\end{aligned}
$$

We show $\mathscr{Z}_1$ is a contraction and $\mathscr{Z}_2$ is compact and continuous using the Arzelà-Ascoli theorem. Therefore, by Krasnoselskii's fixed-point theorem, $\mathscr{Z}$ has at least one fixed point in Ω_δ, proving existence.

Remark 1 Ecologically, the existence of a solution ensures that the population dynamics evolve in a biologically meaningful manner without divergence or unrealistic oscillations.

Theorem 3 If assumption (A_1) holds and

$$\frac{L_\Theta}{M(\kappa_1)}\left(\kappa_2(1-\kappa_1)T^{\kappa_2-1}+\kappa_1 T^{\kappa_2}\right)<1,$$

then by Banach's fixed-point theorem, problem (11) has a unique solution.

Proof. For $t\in\mathbb{I}$, $\vartheta_1,\ \vartheta_2\in\Omega_\delta$. We have

$$|\mathscr{Z}\vartheta_1(t)-\mathscr{Z}\vartheta_2(t)|\ \leq\frac{(1-\kappa_1)}{M(\kappa_1)}\kappa_2 t^{\kappa_2-1}|\Theta(t,\ \vartheta_1(t))-\Theta(t,\ \vartheta_2(t))|$$

$$+\frac{\kappa_1\kappa_2}{\mathbb{M}(\kappa_2)}\int_0^t\omega^{\kappa_2-1}|\Theta(\omega,\ \vartheta_1(\omega))-\Theta(\omega,\ \vartheta_2(\omega))|\,d\omega.$$

Applying assumption (A_1), we obtain

$$|\mathscr{Z}\vartheta_1(t)-\mathscr{Z}\vartheta_2(t)|\leq\frac{(1-\kappa_1)L_\Theta}{M(\kappa_1)}\kappa_2 t^{\kappa_2-1}|\vartheta_1(t)-\vartheta_2(t)|+\frac{\kappa_1 L_\Theta T^{\kappa_2}}{M(\kappa_1)}|\vartheta_1(t)-\vartheta_2(t)|.$$

Taking maximum over the interval $\mathbb{I}$, we have

$$\max_{t\in\mathbb{I}}|\mathscr{Z}\vartheta_1(t)-\mathscr{Z}\vartheta_2(t)|\leq\max_{t\in\mathbb{I}}\left[\frac{(1-\kappa_1)L_\Theta}{M(\kappa_1)}\kappa_2 t^{\kappa_2-1}|\vartheta_1(t)-\vartheta_2(t)|+\frac{\kappa_1 L_\Theta T^{\kappa_2}}{M(\kappa_1)}|\vartheta_1(t)-\vartheta_2(t)|\right].$$

This implies that

$$\|\mathscr{Z}\vartheta_1-\mathscr{Z}\vartheta_2\|\leq\frac{L_\Theta}{M(\kappa_1)}\left(\kappa_2(1-\kappa_1)T^{\kappa_2-1}+\kappa_1 T^{\kappa_2}\right)\|\vartheta_1-\vartheta_2\|.$$

Where $\frac{L_\Theta}{M(\kappa_1)}\left(\kappa_2(1-\kappa_1)T^{\kappa_2-1}+\kappa_1 T^{\kappa_2}\right)<1$. The inequality ensures $\mathscr{Z}$ is a contraction on $\mathfrak{B}$, hence Banach's fixed-point theorem guarantees the uniqueness of the solution.

Remark 2 The uniqueness result corresponds to ecological predictability, meaning that similar initial conditions lead to similar long-term outcomes.

5. Numerical solution

In this section, we aim to find a numerical solution for model (1) under Fractal-Fractional with Caputo-Fabrizio Derivatives (FFCFDs). To develop the numerical scheme for the proposed model, we use the extended Adams-Bashforth-Moulton (ABM) methods with Lagrange interpolation as used in [27]. To go ahead, we write the model as:

$$\begin{cases}{}^{\mathrm{FFCF}}D^{\kappa_1}\Phi(t) &= \kappa_2 t^{\kappa_2-1}g_1(t,\ \Phi(t),\ \Psi(t)),\\ {}^{\mathrm{FFCF}}D^{\kappa_1}\Psi(t) &= \kappa_2 t^{\kappa_2-1}g_2(t,\ \Phi(t),\ \Psi(t)).\end{cases}\tag{22}$$

Using the CF fractional integral, we have

$$\begin{cases} \Phi(t) = \Phi(0) + \dfrac{\kappa_2 t^{\kappa_2-1}(1-\kappa_1)}{\mathscr{M}(\kappa_1)} g_1(t,\, \Phi(t),\, \Psi(t)) + \dfrac{\kappa_1\kappa_2}{\mathscr{M}(\kappa_1)} \int_0^t s^{\kappa_2-1} g_1(s,\, \Phi(s),\, \Psi(s))ds, \\ \Psi(t) = \Psi(0) + \dfrac{\kappa_2 t^{\kappa_2-1}(1-\kappa_1)}{\mathscr{M}(\kappa_1)} g_2(t,\, \Phi(t),\, \Psi(t)) + \dfrac{\kappa_1\kappa_2}{\mathscr{M}(\kappa_1)} \int_0^t s^{\kappa_2-1} g_2(s,\, \Phi(s),\, \Psi(s))ds. \end{cases} \tag{23}$$

At $t = t_{a+1}$, the scheme is given by:

$$\begin{cases} \Phi^{a+1} = \Phi(0) + \dfrac{\kappa_2(1-\kappa_1)t_a^{\kappa_2-1} g_1(t_a,\, \Phi,\, \Psi)}{M(\kappa_1)} + \dfrac{\kappa_1\kappa_2}{M(\kappa_1)} \int_0^{t_a} s^{\kappa_1-1} g_1(s,\, \Phi,\, \Psi)ds, \qquad t_a \in \mathbb{I}, \\ \Psi^{a+1} = \Psi(0) + \dfrac{\kappa_2(1-\kappa_1)t_a^{\kappa_2-1} g_3(t_a,\, \Phi,\, \Psi)}{M(\kappa_1)} + \dfrac{\kappa_1\kappa_2}{M(\kappa_1)} \int_0^{t_a} s^{\kappa_1-1} g_3(s,\, \Phi,\, \Psi)ds, \qquad t_a \in \mathbb{I}. \end{cases} \tag{24}$$

Now take the difference between the consecutive terms, we get

$$\begin{cases} \Phi^{a+1} = \begin{cases} \Phi(0) + \dfrac{\kappa_2(1-\kappa_1)t_a^{\kappa_2-1} g_1(t_a,\, \Phi^a,\, \Psi^a)}{M(\kappa_1)} - \dfrac{\kappa_2(1-\kappa_1)t_{a-1}^{\kappa_2-1} g_1(t_{a-1},\, \Phi^{a-1},\, \Psi^{a-1})}{M(\kappa_1)} \\ + \dfrac{\kappa_1\kappa_2}{M(\kappa_1)} \int_{t_a}^{t_{a+1}} s^{\kappa_1-1} g_1(s,\, \Phi,\, \Psi)ds, \qquad t_a,\, t_{a+1} \in \mathbb{I}, \end{cases} \\ \Psi^{a+1} = \begin{cases} \Psi(0) + \dfrac{\kappa_2(1-\kappa_1)t_a^{\kappa_2-1} g_3(t_a,\, \Phi^a,\, \Psi^a)}{M(\kappa_1)} - \dfrac{\kappa_2(1-\kappa_1)t_{a-1}^{\kappa_2-1} g_3(t_{a-1},\, \Phi^{a-1},\, \Psi^{a-1})}{M(\kappa_1)} \\ + \dfrac{\kappa_1\kappa_2}{M(\kappa_1)} \int_{t_a}^{t_{a+1}} s^{\kappa_1-1} g_3(s,\, \Phi,\, \Psi)ds, \qquad t_a,\, t_{a+1} \in \mathbb{I}. \end{cases} \end{cases} \tag{25}$$

Integrating, and employing Lagrangian interpolation for approximating the kernels, we get

$$\begin{cases} \Phi^{a+1} = \begin{cases} \Phi(0) + \dfrac{\kappa_2(1-\kappa_1)t_a^{\kappa_2-1} g_1(t_a,\, \Phi^a,\, \Psi^a)}{M(\kappa_1)} - \dfrac{\kappa_2(1-\kappa_1)t_{a-1}^{\kappa_2-1} g_1(t_{a-1},\, \Phi^{a-1},\, \Psi^{a-1})}{M(\kappa_1)} \\ + \dfrac{\kappa_2\kappa_1}{M(\kappa_1)} \dfrac{3}{2} (\Delta t) t_a^{\kappa_2-1} g_1(t_a,\, \Phi^a,\, \Psi^a) - \dfrac{\kappa_2\kappa_1}{M(\kappa_1)} \dfrac{(\Delta t)}{2} t_{a-1}^{\kappa_2-1} g_1(t_{a-1},\, \Phi^{a-1},\, \Psi^{a-1}), \\ t_a,\, t_{a-1} \in \mathbb{I}, \end{cases} \\ \Psi^{a+1} = \begin{cases} \Psi(0) + \dfrac{\kappa_2(1-\kappa_1)t_a^{\kappa_2-1} g_3(t_a,\, \Phi^a,\, \Psi^a)}{M(\kappa_1)} - \dfrac{\kappa_2(1-\kappa_1)t_{a-1}^{\kappa_2-1} g_3(t_{a-1},\, \Phi^{a-1},\, \Psi^{a-1})}{M(\kappa_1)} \\ + \dfrac{\kappa_2\kappa_1}{M(\kappa_1)} \dfrac{3}{2} (\Delta t) t_a^{\kappa_2-1} g_3(t_a,\, \Phi^a,\, \Psi^a) - \dfrac{\kappa_2\kappa_1}{M(\kappa_1)} \dfrac{(\Delta t)}{2} t_{a-1}^{\kappa_2-1} g_3(t_{a-1},\, \Phi^{a-1},\, \Psi^{a-1}), \\ t_a,\, t_{a-1} \in \mathbb{I}. \end{cases} \end{cases} \tag{26}$$

Below, we present the numerical algorithm in a more structured pseudocode form.

Algorithm 1 Fractal-Fractional Adams-Bashforth (CF) for model (1)-single order

1. **Input:** $r,\ a,\ b,\ m,\ \varsigma,\ h,\ c,\ d,\ q$; fractional order $\kappa \in (0,\ 1]$; fractal dimension $s \in (0,\ 1]$; normalizing constant M; step size Δt; final time T; initial states $\Phi_0,\ \Psi_0$.
2. Set $N = \lceil T/\Delta t \rceil$, $t_0 = 0$.
3. Precompute:

$$A_1 = s\Big(\frac{1-\kappa}{M} + \frac{3\kappa\Delta t}{2M}\Big), \qquad A_2 = s\Big(\frac{1-\kappa}{M} + \frac{\kappa\Delta t}{2M}\Big).$$

4. Define $f_\Phi(t,\ \Phi,\ \Psi) = r\Phi(1-\Phi/\varsigma) - \dfrac{a\Phi\Psi}{1+h\Phi} + \mathscr{P}(\Phi)$ and $f_\Psi(t,\ \Phi,\ \Psi) = \dfrac{b\Phi\Psi}{1+h\Phi} - m\Psi + \mathscr{Q}(\Psi)$.
5. **Startup (modified euler):** compute $(\Phi_1,\ \Psi_1)$ and $(\Phi_2,\ \Psi_2)$ with two steps of Euler's method.
6. **for** $i = 3$ to $N-1$ **do**
7. $\quad t_{i+1} = t_i + \Delta t$
8. $\quad \Phi_{i+1} = \Phi_i + A_1 t_i^{s-1} f_\Phi(t_i,\ \Phi_i,\ \Psi_i) - A_2 t_{i-1}^{s-1} f_\Phi(t_{i-1},\ \Phi_{i-1},\ \Psi_{i-1})$
9. $\quad \Psi_{i+1} = \Psi_i + A_1 t_i^{s-1} f_\Psi(t_i,\ \Phi_i,\ \Psi_i) - A_2 t_{i-1}^{s-1} f_\Psi(t_{i-1},\ \Phi_{i-1},\ \Psi_{i-1})$
10. **end for**
11. **Output:** $\{t_i,\ \Phi_i,\ \Psi_i\}_{i=0}^{N}$.

Remark 3 The presented algorithm implements a two-step fractal-fractional Adams-Bashforth method formulated in the CF sense. This approach effectively combines the non-singular exponential kernel of the CF derivative with fractal scaling factors, enabling a realistic description of systems that exhibit both memory and heterogeneous geometric effects. The initial steps are computed using a modified Euler scheme, ensuring numerical stability and providing accurate starting values for the multi-step integration process.

Advantages:

• The method is explicit, computationally efficient, and straightforward to implement.

• It avoids the singular kernel of classical fractional derivatives, reducing computational complexity.

• The fractal correction terms allow flexible adjustment to capture irregular biological dynamics.

• The algorithm provides smooth and stable trajectories for both prey and predator populations even under small immigration perturbations.

Limitations:

• The accuracy of the method is step-size dependent; excessively large may cause local instability.

• Being an explicit method, it is conditionally stable and may require finer time steps for stiff systems.

• The CF derivative's limited memory horizon may underestimate long-term historical effects.

Overall, this numerical scheme is well-suited for simulating nonlinear systems governed by fractal-fractional operators.

6. Simulated results with discussion

In this part of the study, we apply the fractal-fractional Adam-Bashforth scheme formulated in the CF framework [37] to simulate and analyze the behavior of the model given in equation (1). The simulations are carried out using MATLAB-R2024a software. In population dynamics, the phenomena of persistence and extinction represent two contrasting outcomes. Traditional predator-prey models illustrate that the oscillatory interaction between predator and prey tends to persist indefinitely. If the prey species disappears, the predator population inevitably collapses due to the lack of food. However, the reverse is not necessarily true; prey can survive and even increase in the absence of predators. The classical models mainly yield cyclic solutions with no tendency towards a stable equilibrium. Despite this, real-world ecological systems often display stable coexistence between predators and prey. Recent investigations have demonstrated that the

presence of a small number of migrants-either predators or prey-can lead to asymptotic stability in such systems. These rare but stable ecological configurations are frequently sustained by limited migration within the predator-prey framework. In the following discussion, we explore three specific scenarios. For all cases, the initial conditions are set as $\Phi(0) = 5$ and $\Psi(0) = 5$. The system parameters are selected based on the values reported in [34]: $r = 0.1$, $a = 0.1$, $b = 0.3$, and $m = 0.2$. Moreover, we set the carrying capacity $\varsigma = 1,000$.

Here, we mention that all the simulations were performed using MATLAB R2024a on a machine with an Intel(R) Core(TM) i5-8350U CPU @ 1.70/1.90 GHz and 16 GB of RAM. Using a step size of $h = 0.01$ and a final simulation time of $t = 5,000$, the proposed ABM numerical scheme required an average CPU time of approximately 0.6944 seconds per figure, based on multiple runs.

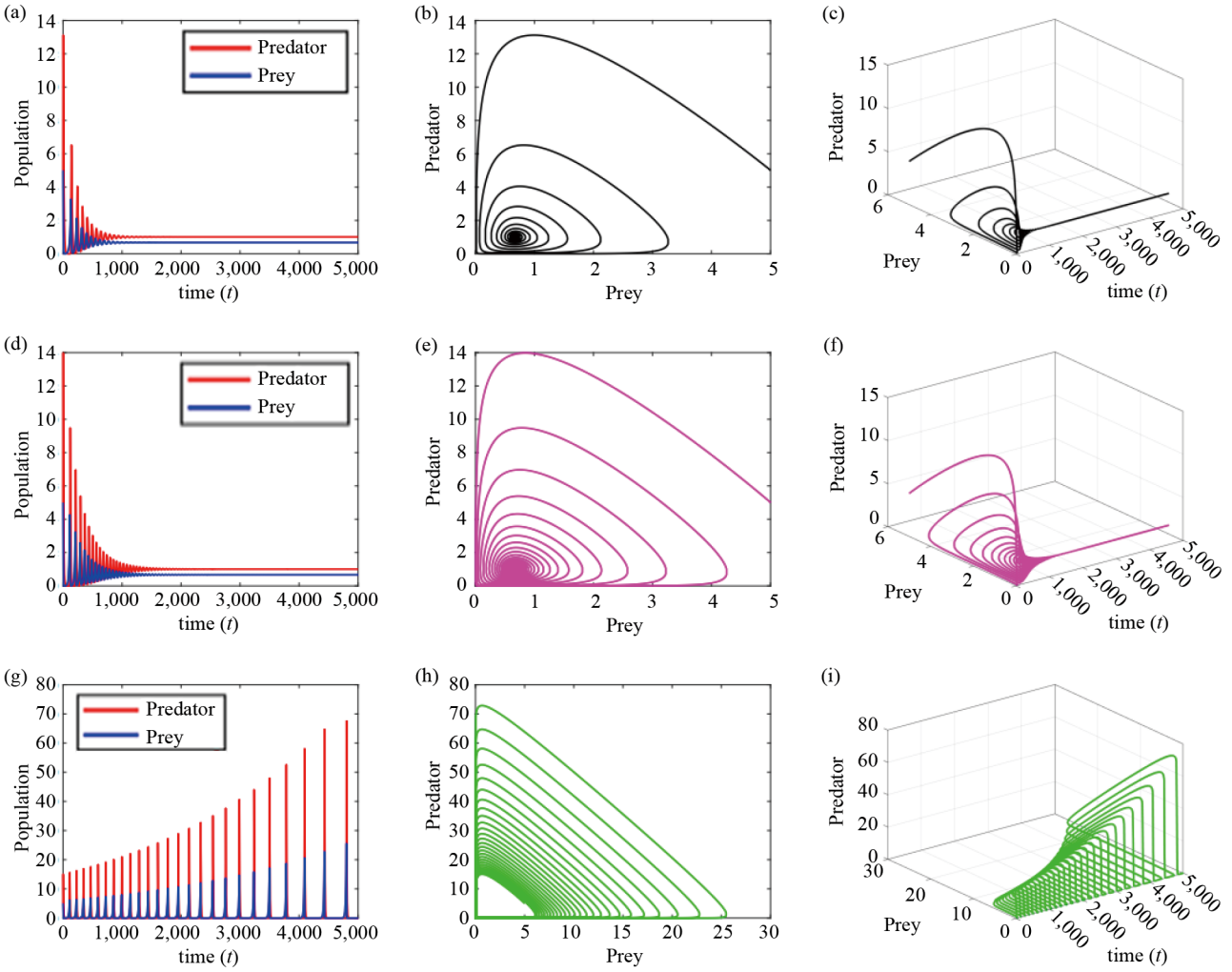

Figure 1. Time-series dynamics of predator-prey populations and the corresponding 2D/3D phase portraits under different fractional orders in the absence of immigration. (a) The population dynamics of predator-prey system for $\kappa_1 = 0.6,\ \kappa_2 = 1.0$; (b) 2D phase portrait of the predator-prey system for $\kappa_1 = 0.6,\ \kappa_2 = 1.0$; (c) 3D phase portrait of predator-prey dynamics over time for $\kappa_1 = 0.6,\ \kappa_2 = 1.0$; (d) The population dynamics of predator-prey system for $\kappa_1 = 0.8,\ \kappa_2 = 1.0$; (e) 2D phase portrait of the predator-prey system for $\kappa_1 = 0.8,\ \kappa_2 = 1.0$; (f) 3D phase portrait of predator-prey dynamics over time for $\kappa_1 = 0.8,\ \kappa_2 = 1.0$; (g) The population dynamics of predator-prey system for $\kappa_1 = 1.0,\ \kappa_2 = 1.0$; (h) 2D phase portrait of the predator-prey system for $\kappa_1 = 1.0,\ \kappa_2 = 1.0$; (i) 3D phase portrait of predator-prey dynamics over time for $\kappa_1 = 1.0,\ \kappa_2 = 1.0$

Case 1: To begin our analysis, we numerically solve the model described in equation (1) without considering any immigration, meaning $\mathscr{P}(\Phi) = 0$ and $\mathscr{Q}(\Psi) = 0$, across multiple fractional orders and with a fractal order set to 1.0. The

outcomes are visualized in Figure 1, which presents the population dynamics of both predator and prey, along with the corresponding phase portraits, for the given fractional and fractal orders under the assumption of no immigration.

Further insights are illustrated in Figures 1a-c, which correspond to the dynamics and phase space trajectories for $\kappa_1 = 0.6$ and $\kappa_2 = 1.0$. Similarly, Figures 1d-f demonstrate the behavior for $\kappa_1 = 0.8$ and $\kappa_2 = 1.0$. For the scenario with both orders equal to one ($\kappa_1 = \kappa_2 = 1.0$), the resulting dynamics and phase spaces are shown in Figures 1g-i.

From these illustrations, it becomes evident that in the absence of immigration, the system exhibits instability. However, under fractional and fractal-fractional derivative settings (e.g., in Figures 1a, b), there is evidence of population stabilization over time. In contrast, the classical derivative model fails to show such stability. This highlights the enhanced stability and flexibility of fractional and fractal-fractional operators compared to standard integer-order derivatives.

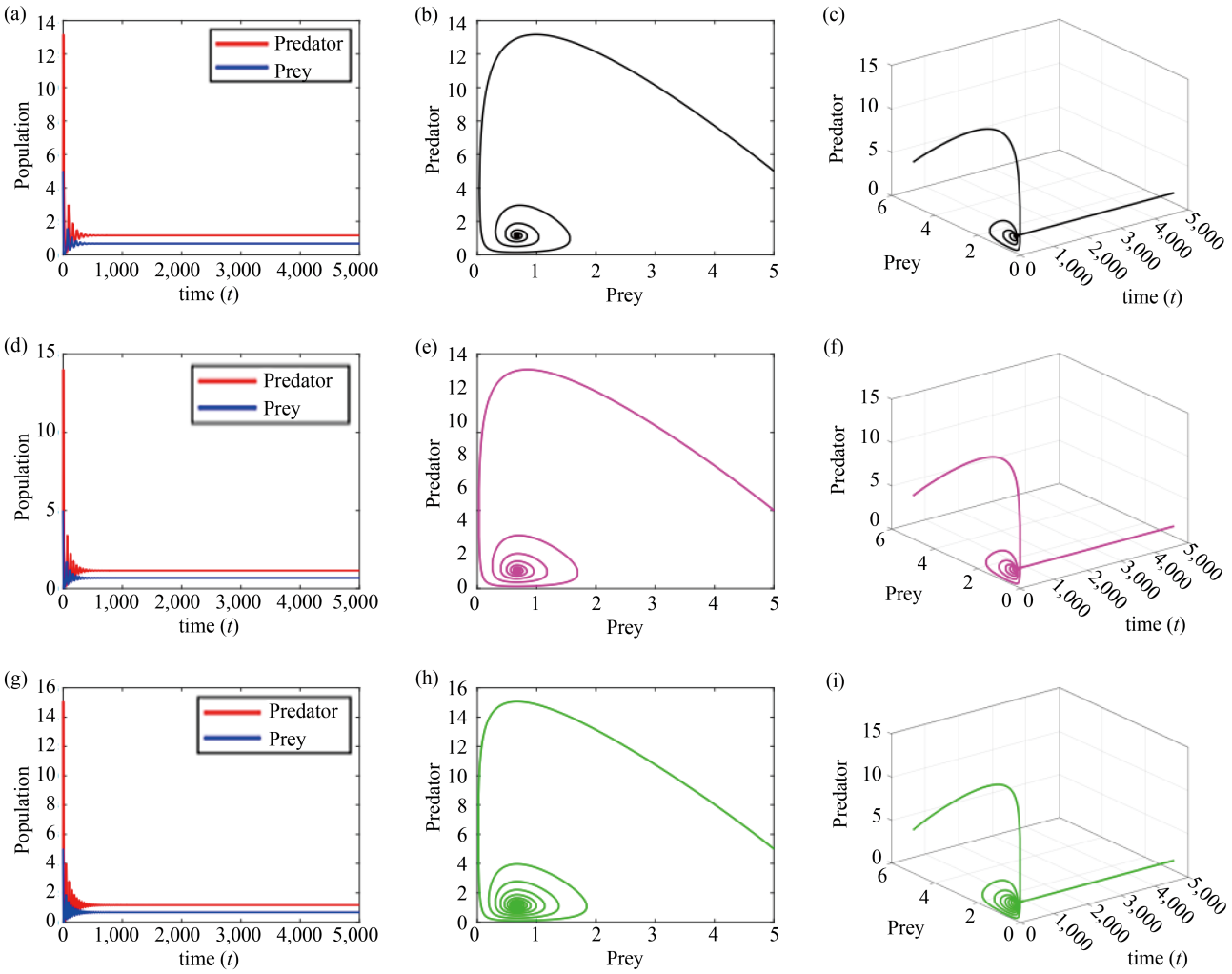

Figure 2. Time-series dynamics of predator-prey populations and the corresponding 2D/3D phase portraits under different fractional orders and $\mathscr{P}(\Phi) = 0.01$. (a) The population dynamics of predator-prey system for $\kappa_1 = 0.6,\ \kappa_2 = 1.0$; (b) 2D phase portrait of the predator-prey system for $\kappa_1 = 0.6,\ \kappa_2 = 1.0$; (c) 3D phase portrait of predator-prey dynamics over time for $\kappa_1 = 0.6,\ \kappa_2 = 1.0$; (d) The population dynamics of predator-prey system for $\kappa_1 = 0.8,\ \kappa_2 = 1.0$; (e) 2D phase portrait of the predator-prey system for $\kappa_1 = 0.8,\ \kappa_2 = 1.0$; (f) 3D phase portrait of predator-prey dynamics over time for $\kappa_1 = 0.8,\ \kappa_2 = 1.0$; (g) The population dynamics of predator-prey system for $\kappa_1 = 1.0,\ \kappa_2 = 1.0$; (h) 2D phase portrait of the predator-prey system for $\kappa_1 = 1.0,\ \kappa_2 = 1.0$; (i) 3D phase portrait of predator-prey dynamics over time for $\kappa_1 = 1.0,\ \kappa_2 = 1.0$

Case 2: In this case, we introduce a constant influx of prey immigrants into the system. Specifically, we set $\mathscr{P}(\Phi) = x = 0.01$, and conduct numerical experiments on the model. The goal is to observe how this addition influences the dynamics of both prey and predator populations under various fractional orders while keeping the fractal dimension

constant. The simulation results are presented in Figure 2, which illustrates the time evolution and phase portraits of the system under these conditions.

An examination of Figure 2 reveals that introducing a constant prey immigration rate, $\mathscr{P}(\Phi) = x = 0.01$, leads to gradual asymptotic stabilization of both predator and prey populations under various fractional orders and a fixed fractal dimension. In contrast, under the classical (integer-order) framework, population stabilization occurs more rapidly, reaching equilibrium in approximately 700 days.

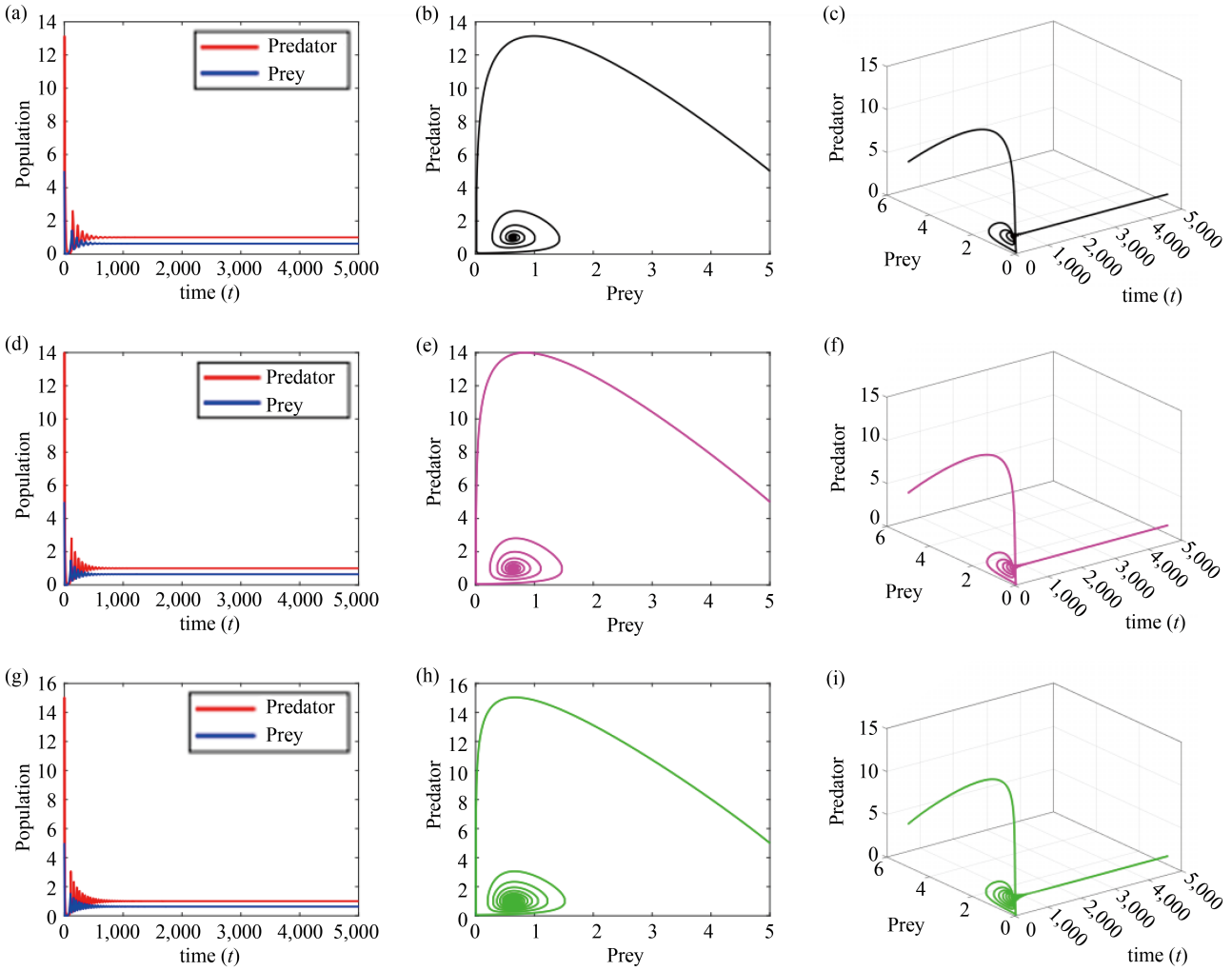

Figure 3. Time-series dynamics of predator-prey populations and the corresponding 2D/3D phase portraits under different fractional orders and $\mathscr{Q}(\Psi) = 0.01$. (a) The population dynamics of predator-prey system for $\kappa_1 = 0.6,\ \kappa_2 = 1.0$; (b) 2D phase portrait of the predator-prey system for $\kappa_1 = 0.6,\ \kappa_2 = 1.0$; (c) 3D phase portrait of predator-prey dynamics over time for $\kappa_1 = 0.6,\ \kappa_2 = 1.0$; (d) The population dynamics of predator-prey system for $\kappa_1 = 0.8,\ \kappa_2 = 1.0$; (e) 2D phase portrait of the predator-prey system for $\kappa_1 = 0.8,\ \kappa_2 = 1.0$; (f) 3D phase portrait of predator-prey dynamics over time for $\kappa_1 = 0.8,\ \kappa_2 = 1.0$; (g) The population dynamics of predator-prey system for $\kappa_1 = 1.0,\ \kappa_2 = 1.0$; (h) 2D phase portrait of the predator-prey system for $\kappa_1 = 1.0,\ \kappa_2 = 1.0$; (i) 3D phase portrait of predator-prey dynamics over time for $\kappa_1 = 1.0,\ \kappa_2 = 1.0$

Case 3: In this case, we introduce a constant influx of predator immigrants into the system. Specifically, we set $\mathscr{Q}(\Psi) = x = 0.01$, and assume no prey immigration, i.e., $\mathscr{P}(\Phi) = 0$. We conduct numerical experiments on the model for these conditions under different fractional orders and a fixed fractal dimension. Figure 3 illustrates the evolution of both predator and prey populations, along with their phase space trajectories, under the influence of this low-level predator immigration.

Further details are provided in Figures 3a-c, which show the dynamics for the case $\kappa_1 = 0.6$ and $\kappa_2 = 1.0$. Similarly, Figures 3d-f present the population and phase space behavior for $\kappa_1 = 0.8$ and $\kappa_2 = 1.0$. Lastly, the dynamics for the classical derivative scenario with $\kappa_1 = \kappa_2 = 1.0$ are depicted in Figures 3g-i.

From the analysis of Figure 3, it is evident that introducing predator immigrants at a constant rate, $\mathscr{Q}(\Psi) = z = 0.01$, leads to asymptotic stabilization of both populations over time under various fractional orders and a fixed fractal dimension-although this stabilization occurs rather slowly. In contrast, in the classical (integer-order) case, the system achieves stability in approximately 1,500 days.

The results imply that increasing the number of immigrants in either population can significantly enhance the rate at which the system stabilizes. Therefore, introducing a sufficient number of individuals into the predator or prey population can drive the predator-prey system toward asymptotic stability. However, such an outcome is contingent on the habitat being favorable to immigration-meaning that environmental conditions must support and attract incoming individuals. In the case of density-dependent immigration (e.g., $\mathscr{Q}(\Psi) = z/\Psi$), the number of immigrants decreases as the population grows, which reflects a realistic ecological constraint, such as carrying capacity. Although these two immigration schemes differ biologically, both lead to long-term stabilization of the system.

We give the overall significance of numerical results as below:

• Fractional and fractal-fractional derivatives introduce memory that naturally enhances ecosystem stability.

• Immigration, even at very low levels, acts as an ecological buffer preventing extinction events.

• Density-dependent inflows provide a realistic mechanism where stabilization occurs slowly but sustainable.

7. Conclusion and future research

In this work, we developed a novel fractal-fractional predator-prey model incorporating logistic growth and immigration effects, employing the CF operator to capture memory and hereditary characteristics inherent in biological systems. The use of a nonlinear Holling type II functional response enabled the model to realistically depict saturation effects in predator-prey interactions, thereby overcoming the limitations of linear predation assumptions. By applying the Krasnoselskii's fixed point theorem and Banach's contraction principle, we established the existence and uniqueness of solution for the proposed system.

Numerical simulations based on a fractal-fractional Adams-Bashforth method adapted to the CF framework demonstrated that small but positive immigration rates play a stabilizing role in predator-prey dynamics. Specifically, sporadic immigration contributes to asymptotic stability, maintaining coexistence and preventing population collapse. These findings underscore the ecological relevance of external influxes in sustaining biodiversity and ecosystem resilience.

Despite its effectiveness, the present study has certain limitations. The model assumes homogeneous environmental conditions and constant parameter values, which may not fully capture spatial heterogeneity, seasonal variations, or stochastic environmental effects.

Future research could extend the current framework by incorporating stochastic perturbations, time-delay effects, or spatial diffusion to investigate pattern formation and spatial stability. Additionally, exploring the impact of variable fractional and fractal orders could provide deeper insights into how memory intensity and geometric complexity affect long-term ecosystem dynamics. Such extensions would enhance the realism and applicability of the proposed model to more complex ecological scenarios.

Funding

This research has been funded by Scientific Research Deanship at University of Hail-Saudi Arabia through project number RG-25 026.

Data availability statement

The references are given in the paper about the data.

Conflict of interest

The authors declare no competing financial interest.

References

[1] Naji RK, Mustafa AN. The dynamics of an eco-epidemiological model with nonlinear incidence rate. *Journal of Applied Mathematics*. 2012. Available from: https://doi.org/10.1155/2012/852631.

[2] Shi C, Chen X, Wang Y. Feedback control effect on the Lotka-Volterra prey-predator system with discrete delays. *Advances in Difference Equations*. 2017; 2017: 373.

[3] Aboites V, Bravo-Avilés JF, García-López JH, Jaimes-Reategui R, Huerta-Cuellar G. Interpretation and dynamics of the Lotka-Volterra model in the description of a three-level laser. *Photonics*. 2022; 9(1): 16.

[4] Liu J, Zhao W. Dynamic analysis of stochastic Lotka-Volterra predator-prey model with discrete delays and feedback control. *Complexity*. 2019. Available from: https://doi.org/10.1155/2019/4873290.

[5] Pérez JFS, Conesa M, Alhama I, Cánovas M. Study of Lotka-Volterra biological or chemical oscillator problem using the normalization technique: prediction of time and concentrations. *Mathematics*. 2020; 8: 1324.

[6] Bacaër N. McKendrick and Kermack on epidemic modelling (1926-1927). In: *A Short History of Mathematical Population Dynamics*. London: Springer; 2011. p.89-96.

[7] Hudson PJ, Dobson AP, Newborn D. Do parasites make prey vulnerable to predation? Red grouse and parasites. *Journal of Animal Ecology*. 1992; 61(3): 681-692.

[8] Pal AK, Samanta GP. Stability analysis of an eco-epidemiological model incorporating a prey refuge. *Nonlinear Analysis: Modelling and Control*. 2010; 15(4): 473-491.

[9] Mukhopadhyay B, Bhattacharyya R. Role of predator switching in an eco-epidemiological model with disease in the prey. *Ecological Modelling*. 2009; 220(7): 931-939.

[10] Das KP, Roy S, Chattopadhyay J. Effect of disease-selective predation on prey infected by contact and external sources. *BioSystems*. 2009; 95(3): 188-199.

[11] Sinha S, Misra OP, Dhar J. Study of a prey-predator dynamics under the simultaneous effect of toxicant and disease. *Journal of Nonlinear Science and Applications*. 2008; 1(2): 102-117.

[12] Xiao Y, Chen L. A ratio-dependent predator-prey model with disease in the prey. *Applied Mathematics and Computation*. 2002; 131(2-3): 397-414.

[13] Díaz-Pitá E, Ortiz-Espinar MV. Predator-prey models: a review of some recent advances. *Mathematics*. 2021; 9: 1783.

[14] Bohannan GW. Analog fractional order controller in temperature and motor control applications. *Journal of Vibration and Control*. 2008; 14(9-10): 1487-1498.

[15] Krishna BT, Reddy KVVS. Active and passive realization of fractance device of order 1/2. *Active and Passive Electronic Components*. 2008. Available from: https://doi.org/10.1155/2008/369421.

[16] Lima MFM, Machado JAT, Crisóstomo M. Experimental signal analysis of robot impacts in a fractional calculus perspective. *Journal of Advanced Computational Intelligence and Intelligent Informatics*. 2007; 11(9): 1079-1085.

[17] De Espíndola J, Bavastri C, Lopes EDO. Design of optimum systems of viscoelastic vibration absorbers based on the fractional calculus model. *Journal of Vibration and Control*. 2008; 14(9-10): 1607-1630.

[18] Magin RL, Ovadia M. Modeling the cardiac tissue electrode interface using fractional calculus. *Journal of Vibration and Control*. 2008; 14(9-10): 1431-1442.

[19] Khan ZA, Ali A, Irshad AUR, Ozdemir B, Alrabaiah H. On theoretical and numerical results of serum hepatitis disease using piecewise fractal-fractional perspectives. *Fractal and Fractional*. 2024; 8: 260.

[20] Ali Z, Rabiei F, Rashidi MM, Khodadadi T. A fractional-order mathematical model for COVID-19 outbreak with symptomatic and asymptomatic transmissions. *European Physical Journal Plus*. 2022; 137: 395.

[21] Alraqad T, Almalahi MA, Mohammed N, Alahmade A, Aldwoah KA. Modeling Ebola dynamics with a Φ-piecewise hybrid fractional derivative approach. *Fractal and Fractional*. 2024; 8(10): 596.
[22] Youssri YH, Hafez RM, Atta AG. An innovative pseudo-spectral Galerkin algorithm for the time-fractional Tricomi-type equation. *Physica Scripta*. 2024; 99(10): 105238.
[23] Youssri YH, Atta AG. Chebyshev Petrov-Galerkin method for nonlinear time-fractional integro-differential equations with a mildly singular kernel. *Journal of Applied Mathematics and Computing*. 2025; 71: 3891-3911.
[24] Abd-Elhameed WM, Al-Sady AM, Alqubori OM, Atta AG. Numerical treatment of the fractional Rayleigh-Stokes problem using orthogonal combinations of Chebyshev polynomials. *AIMS Mathematics*. 2024; 9(9): 25457-25481.
[25] Yousef F, Semmar B, Al Nasr K. Dynamics and simulations of discretized Caputo-conformable fractional-order Lotka-Volterra models. *Nonlinear Engineering*. 2022; 11: 100-111.
[26] Elsonbaty A, Elsadany AA. On discrete fractional-order Lotka-Volterra model based on the Caputo difference operator. *Mathematical Sciences*. 2021. Available from: https://doi.org/10.1007/s40096-021-00442-0.
[27] Jafari H, Ganji RM, Nkomo NS, Lvd YP. A numerical study of fractional order population dynamics model. *Results in Physics*. 2021; 27: 104456.
[28] Atangana A. Fractal-fractional differentiation and integration: connecting fractal calculus and fractional calculus to predict complex system. *Chaos, Solitons and Fractals*. 2017; 102: 396-406.
[29] Imran MA. Application of fractal fractional derivative with power-law kernel to MHD viscous fluid flow. *Chaos, Solitons and Fractals*. 2020; 134: 109691.
[30] Aslam M, Farman M, Ahmad H, Gia TN, Ahmad A, Askar S. Fractal fractional derivative on chemistry kinetics hires problem. *AIMS Mathematics*. 2022; 7(1): 1155-1184.
[31] Hamza AE. Fractal-fractional modeling of liver fibrosis disease and mathematical results with subinterval transitions. *Fractal and Fractional*. 2024; 8(11): 638.
[32] Khan H, Alzabut J, Shah A, He ZY, Etemad S, Rezapour S, Zada A. On a fractal-fractional waterborne disease model: theoretical and numerical aspects via simulations. *Fractals*. 2023; 31(4): 2340055.
[33] Li Z, Liu Z, Khan MA. Fractional investigation of bank data with fractal-fractional Caputo derivative. *Chaos, Solitons and Fractals*. 2020; 131: 109528.
[34] Tahara T, Gavina MKA, Kawano T. Asymptotic stability of a modified Lotka-Volterra model with small immigrations. *Scientific Reports*. 2018; 8: 1-7.
[35] Ali Z, Rabiei F, Hosseini K. A fractal-fractional-order modified predator-prey model with immigrations. *Mathematics and Computers in Simulation*. 2023; 207: 466-481.
[36] Burton TA. A fixed-point theorem of Krasnoselskii. *Applied Mathematics Letters*. 1998; 11: 85-88.
[37] Atangana A, Khan MA, Fatmawati. Modeling and analysis of competition model of bank data with fractal-fractional Caputo-Fabrizio operator. *Alexandria Engineering Journal*. 2020; 59(40): 1985-1998.